MAPPING OF CRACK EDGES BY SEISMIC METHODS

By J. D. Achenbach, A. Norris, and K. Viswanathan*

ABSTRACT

The inverse problem of diffraction of elastic waves by the edge of a large crack has been investigated on the basis of elastodynamic ray theory and the geometrical theory of diffraction. Two methods are discussed for the mapping of the edge of a crack-like flaw in an elastic medium. The methods require as input data the arrival times of diffracted ultrasonic signals. The first method maps flash points on the crack edge by a process of triangulation with the source and receiver as given vertices of the triangle. By the use of arrival times at neighboring positions of the source and/or the receiver, the directions of signal propagation, which determine the triangle, can be computed. This inverse mapping is global in the sense that no a priori knowledge of the location of the crack edge is necessary. The second method is a local edge mapping which determines planes relative to a known point close to the crack edge. Each plane contains a flash point. The envelope of the planes maps an approximation to the crack edge. The errors due to inaccuracies in the input data and in the computational procedure have been illustrated by specific examples.

Introduction

Analytical studies are presented which bear on the feasibility of mapping the edge of a large crack by methods based on edge diffraction of signals emitted by a point source.

The material containing the crack is taken as a homogeneous, isotropic, linearly elastic solid. The proposed methods use travel times of signals which propagate from the source via a point on the crack edge to the receiver. The first diffracted signal that is received satisfies Fermat's principle of least time. Hence, it propagates along a stationary ray path which includes an incident ray from the source to the point of diffraction on the crack edge (the flash point D), and a diffracted ray from D to the receiver. In the direct problem the geometry of the crack edge is known, and the positions of flash points and the associated travel times can be computed by using the rules of geometrical diffraction theory. In this paper we are, however, interested in the inverse problem. We assume that the travel times can be measured and we infer the positions of the flash points. A sufficiently large number of inferred flash points provides an approximation to the crack edge.

Two methods are discussed in this paper. In the first method, which is a global triangulation method, the source and the receiver are the given corner points of a triangle, and the flash point is computed as the third corner point. The triangle may be completed if the direction of the stationary ray path is known at either the source or the receiver. This direction can be computed by measuring the spatial gradient of the travel time. Mathematical details and a fairly detailed error analysis have been given by Norris and Achenbach (1982).

The second method is a local mapping technique. It is local in the sense that a point near the crack edge must be known a priori. This point, however, can be determined by the global triangulation method. The travel times corresponding to several different source-receiver pairs form surfaces on whose intersections the flash

^{*} Present address: Defense Science Laboratory, Delhi-110054, India.

points must be located. To a first approximation, these surfaces can be replaced by planes, whose intersection approximates the crack edge.

Numerical tests of both methods have been carried out by the use of synthetic data. For perfect data, these tests provide illustrations of the errors that are introduced by the computational method. Results of tests with specified induced errors of the synthetic travel times show that the global triangulation method is quite sensitive to inaccuracies of the input data. It may, however, be expected that a point close enough to the crack edge can be obtained to provide a base point for the local crack-edge mapping procedure. An iteration scheme has been developed to improve the accuracy of the local mapping. In a test of the local mapping technique, the synthetic data were perturbed by random errors. For moderate errors, it was found that even though individual flash point positions may deviate substantially from the crack edge, a least-square polynomial fit to all computed flash points still gives good approximation to a segment of the crack edge.

Throughout the paper, the source and receiver have been assumed separate, i.e., the measurement method is pitch-catch. The analysis can easily be modified for an arrangement with an identical source and receiver, to accommodate pulse-echo measurements.

Crack characterization by wave propagation methods has been successful in the field of quantitative nondestructive evaluation of materials, as discussed by Achenbach *et al.* (1979). The difficulties in a geological setting are, however, much greater, primarily because wave propagation in rock and rock formations is more complicated than in metals, and fluid-filled cracks in rock may be weak diffractors of incident waves. In addition, there may be limited options for the placement of transmitters and receivers in boreholes, and the shape of the crack may be quite irregular.

This work was motivated by interest in a method to locate hydraulically induced water-filled cracks in a hot-dry-rock geothermal energy system [Brown et al. (1978)]. When it is possible to vary arbitrarily the positions of sources and receivers, then the edge of a plane crack can be determined by the use of reflection and transmission data. The fracture and wellbore system at the Fenton-Hill site described by Brown et al. (1978) is, however, vertical, and at a depth of between 2500 and 2800 m. It is not useful to place transmitters and receivers at the earth's surface because seismic signals are damped by a thick layer of tuff. Thus, the instrumentation has to be lowered in two boreholes that are part of the geothermal heat-exchange system. As a consequence, the information obtained by reflection and transmission is limited, and it is desirable to supplement it with information from diffraction of seismic waves by the edge of the crack. Diffracted signals generally are of smaller order of magnitude, and hence are best measured at positions where reflected and transmitted signals do not occur. By locating the source and the receiver above the crack edge, the reflected and transmitted signals propagate away from the source and the receiver, and the only signals in addition to the direct signal are pulse-echo and pitch-catch signals diffracted by the crack edge.

It is usually assumed that hydraulic fractures are vertical, since the principal stresses are lowest in horizontal directions. A crack may, however, not be vertical, depending on the local geological configuration. For example, certain hydraulic fractures that have been considered for the disposal of nuclear wastes are located in between layers in horizontal planes. The results presented in this paper may also have application to the mapping of oil-filled cracks, the detection of water-filled crevasses in ice, and the sizing of magma lenses.

The reflection and transmission by empty and fluid-filled cracks of plane longitudinal and transverse waves at various angles of incidence have been studied by Fehler and Aki (1978) in a two-dimensional geometry. Reflection and refraction of purely longitudinal waves incident on a slipping interface was discussed by Salvado and Minster (1980).

EDGE DIFFRACTION

The theory of elastodynamic edge diffraction is based on the result that two cones of diffracted rays are generated when a ray carrying a high-frequency elastic wave strikes the edge of a crack. The inner and outer cones consist of rays of longitudinal and transverse motion, respectively. For cracks in elastic solids, the three-dimensional theory of edge diffraction was discussed by Achenbach and Gautesen (1977).

Figure 1 shows an incident ray of longitudinal motion and the corresponding cones of diffracted rays. The angle of the incident ray with the edge is ϕ_L . Thus



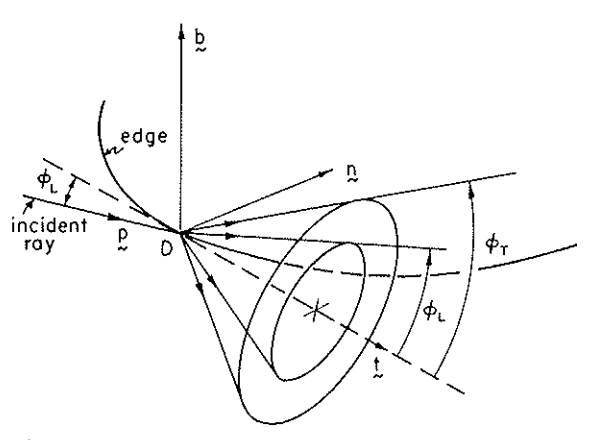


Fig. 1. Propagation vector p of incident ray and cones of diffracted rays at flash point D.

where p defines the direction of propagation along the incident ray and t is a unit vector along the tangent to the edge, chosen in the direction which makes ϕ_L acute. The half-angles ϕ_{β} of the cones of diffracted rays of type $\beta(\beta = L, T)$ are given by ϕ_L and ϕ_T , where

$$\cos \phi_T = (c_T/c_L)\cos \phi_L. \tag{2}$$

For time-harmonic motion and $k_{\beta}R_{\beta}\gg 1$, the field on the diffracted ray of type $\beta=L$, T may be expressed in the form

$$\mathbf{u}^{\beta} = U_0[k_{\beta}R_{\beta}(1 + R_{\beta}/\rho_{\beta})]^{-1/2}D_{\beta}^{L}(\theta; \phi_L, \theta_L)\exp[ik_{\beta}R_{\beta}] \,\mathbf{d}^{\beta}$$
(3)

where U_0 defines the amplitude and phase on the incident ray at the point of diffraction, $D_{\beta}^{L}(\theta; \phi_L, \theta_L)$ is the diffraction coefficient, the angle θ_L follows from cos $\phi_L = \boldsymbol{p} \cdot \boldsymbol{n}/\sin \phi_L$, d^{β} is the unit vector which defines the displacement direction, R_{β} is the distance along a diffracted ray measured from the point of diffraction, and ρ_{β} is the distance from the point of diffraction to the other caustic. An explicit

expression for ρ_{β} is

$$\rho_{\beta} = -a \sin \phi_{\beta} [a \ d\phi_{\beta}/ds + \cos \theta_{L}]^{-1}$$
 (4)

where s is arc length measured along the edge and a is the signed radius of curvature of the edge.

The diffraction coefficient $D_{\beta}^{L}(\theta; \phi_{L}, \theta_{L})$ can be obtained by solving the canonical problem of diffraction of plane waves by a semi-infinite crack. For crack faces which are free of surface tractions (an empty crack) this was done by Achenbach *et al.* (1978). For other conditions on the faces of the crack, a pertinent canonical problem can be solved in the same manner, provided that the conditions on the crack faces define a linear problem.

In the direct problem, the positions of the source and the receiver, which are defined by x_S and x_Q , respectively, are known. Also known is the location of the edge of the crack. The location of the flash point D, with position vector x_D , must be determined. For L-L diffraction, it follows from (1) and (2) that x_D satisfies the relation

$$t \cdot \{|x_D - x_S| (x_Q - x_D) - |x_Q - x_D| (x_D - x_S)\} = 0,$$
 (5)

where the unit vector t is tangent to the edge at $x = x_D$. When the vector x_D has been determined, the total ray length may be computed as

$$R = R_i + R_L$$

= $|x_D - x_S| + |x_Q - x_D|$. (6)

In the time domain, the ray geometry of the incident ray and the cones of diffracted rays, which is shown in Figure 1, is valid for small times after the arrival of a diffracted pulse. In general, a solution in the frequency domain at high frequencies is related to the solution near the wave fronts in the time domain, by well-known rules of Fourier analysis.

GLOBAL TRIANGULATION METHOD

In the inverse problem, the position vectors x_S and x_Q are known. In addition, the time $\tau(x_S, x_Q)$, which denotes the time span between emission at x_S and reception of the diffracted signal at x_Q is known. For L-L diffraction we then also know

$$R = R(\mathbf{x}_S, \mathbf{x}_Q) = c_L \tau(\mathbf{x}_S, \mathbf{x}_Q) \tag{7}$$

where c_L is the speed of longitudinal waves. On the basis of ray theory, it then follows that x_D is located on a spheroid E(x), whose foci are at the points x_S and x_Q , and whose major axis length is R. The eccentricity of the spheroid is

$$e = |x_O - x_S|/R = |X|/R$$
 (8)

where we have implied

$$X = x_O - x_S. (9)$$

MAPPING OF CRACK EDGES BY SEISMIC MELLIOUS

The length of the minor axis is $(1 - e^2)^{1/2}R$, and the semi-latus rectum, l, is

$$l = \frac{1}{2}(1 - e^2)R. \tag{10}$$

", OQ

For any point on the spheroid, we have

$$\boldsymbol{p} = (\boldsymbol{x} - \boldsymbol{x}_{\mathrm{S}})/R_{i} \tag{11a}$$

$$R_i = |x - x_S|. \tag{11b}$$

We also define

$$q = (x - x_Q)/R_L \tag{12a}$$

$$R_L = |\mathbf{x} - \mathbf{x}_Q|. \tag{12b}$$

By using the equation for an ellipse in polar coordinates, centered at x_s , E(x) may be represented by

$$E(x) = \{x \mid x = x_S + R_i \mathbf{p}; R_i = l[1 - e\mathbf{p} \cdot \mathbf{X} / |\mathbf{X}|]^{-1}, |\mathbf{p}| = 1\}.$$
 (13)

The length R_i can also be expressed as

$$R_i = W/2(R - \boldsymbol{p} \cdot \boldsymbol{X}) \tag{14a}$$

where

$$W = R^2 - |X|^2. (14b)$$

Thus, from the travel time (or ray length) from one source position to one receiver position, it can be concluded that the flash point x_D is located on a spheroid with focal points at S and Q. To determine the actual position of the flash point, we need travel times for additional source and/or receiver positions. A large shift of the source and/or the receiver position will give rise to a quite different flash point. The shift of the flash point is, however, of second order when either or both the source and the observer are moved only slightly. This property will be used to determine the positions of flash points.

Let us first move point Q over a small distance in the direction defined by the unit vector V. As x_Q changes, so does the travel distance R and the spheroid E(x). The distance R_i for a point which is on the intersection of the two spheroids satisfies the equation

$$\nabla_{\mathbf{v}} R_i \equiv \mathbf{V} \cdot \nabla R_i = 0. \tag{15}$$

By the use of (14), we then find

$$\mathbf{p} \cdot \nabla_{\mathbf{v}}(\mathbf{X}/\mathbf{W}) - \nabla_{\mathbf{v}}(\mathbf{R}/\mathbf{W}) = 0 \tag{16}$$

where W is defined by (14b). Similarly, if the source is moved over a small distance

in the direction defined by the unit vector U, we find

$$\mathbf{q} \cdot \nabla_{U}(X/W) + \nabla_{U}(R/W) = 0. \tag{17}$$

Additional relations follow by tracing the change of R as the source is moved from S_1 to S_2 , as shown in Figure 2. We have

$$\Delta R = \overline{S_2 D_2} + \overline{D_2 Q} - \overline{S_1 D_1} - \overline{D_1 Q}. \tag{18}$$

To first order this relation can be reduced to

$$\Delta R = -\overline{S_1 S_2} \mathbf{p} \cdot U + \overline{D_1 D_2} \cos(\phi_L + \Delta \phi_L) - D_1 D_2 \cos \phi_L, \tag{19}$$

from which it follows that

$$\mathbf{p} \cdot \mathbf{U} + \nabla_{\mathbf{U}}(R) = 0. \tag{20}$$

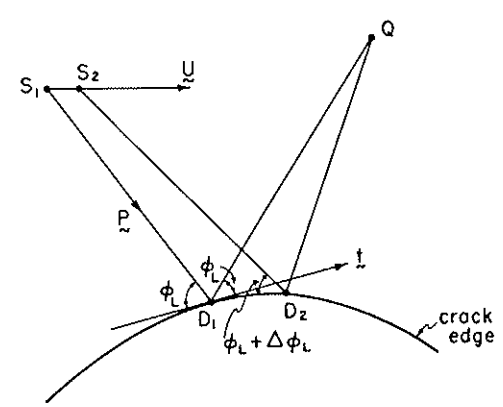


Fig. 2. Receiver position Q, source positions S_1 and S_2 , and corresponding flash points D_1 and D_2 .

In a similar manner we obtain

$$\mathbf{q} \cdot \mathbf{V} + \nabla_{\mathbf{V}}(R) = 0. \tag{21}$$

The system of equations (16) and (17) and (20) and (21) must be supplemented by

$$|\boldsymbol{p}| = 1 \tag{22a}$$

and

$$|q| = 1. (22b)$$

The unit vector p can be solved from (16), (20), and (22a). Equations (16) and (20) represent planes, while (22a) is a unit sphere. The intersection of each plane with the unit sphere provides a circle. The two circles have two points of intersection. The simultaneous equations are of the general form

$$p \cdot a + C_1 = 0;$$
 $p \cdot U + C_2 = 0,$ $|p| = 1$ (23)

where

$$\alpha = \nabla_{\mathbf{V}}(X/W)/|\nabla_{\mathbf{V}}(X/W)|, \qquad W = R^2 - |X|^2$$
(24)

$$C_1 = -\nabla_V(R/W)/|\nabla_V(X/W)| \tag{25}$$

$$C_2 = \nabla_U(R). \tag{26}$$

It is noted that

$$|a| = |U| \equiv 1, \quad -1 \le C_1, C_2 \le 1,$$
 (27)

and we assume that a and U are not parallel. The solution to (23) may be written as

$$p^{\pm} = \{ (C_2 \mathbf{a} - C_1 \mathbf{U}) \wedge (\mathbf{a} \wedge \mathbf{U}) \pm [|\mathbf{a} \wedge \mathbf{U}|^2 - |C_2 \mathbf{a} - C_1 \mathbf{U}|^2]^{1/2} (\mathbf{a} \wedge \mathbf{U}) \} / |\mathbf{a} \wedge \mathbf{U}|^2.$$
(28)

In the same manner, we can solve for q from (17), (21), and (22b). Whether we determine p or q, there will be some ambiguity in the location of the flash point. For example, the point corresponding to p^+ is different from the point for p^- . However, in practice it should be simple to decide which of p^+ or p^- is the correct vector. For instance, if both source and receiver are located on a free surface, then only one of p^+ will point into the solid. Once p has been determined, the position x_D may be expressed as

$$x_D = x_S + R_i \boldsymbol{p}. \tag{29}$$

In summary then, the crack-edge mapping proceeds as follows. We start with a source point S_1 , defined by x_S , and a receiver Q_1 , defined by x_Q . For these two points, we have a total ray length R. We then define unit vectors U and V at S_1 and Q_1 , respectively, and we consider a source point S_2 and a point of observation Q_2 at distances Δu and Δv along U and V, respectively. For the combinations of S_2 and Q_1 and S_1 and S_2 , we then find the total ray lengths from the observed travel times. The new ray lengths can be used to make first order computations of the gradients appearing in (24) to (26). Substitution of the results in (28) yields the position of the flash points corresponding to source S_1 and observer S_2 .

In an alternative method for determining the flash point, the position of the source is kept unchanged, but a total of three receiver positions are employed. In addition to the receiver position Q_1 , we consider positions Q_2 and Q_3 , which are short distances from Q_1 along the unit vectors V_1 and V_2 , respectively, where $V_1 \wedge V_2 \neq 0$. According to equation (16), the unit vector \boldsymbol{p} can then be solved from

$$\mathbf{p} \cdot \nabla_{V_j}(\mathbf{X}/W) - \nabla_{V_j}(R/W) = 0, \qquad j = 1, 2. \tag{30}$$

Here, W is defined by equation (14b). It follows from (21) that the unit vector q can be solved from

$$q \cdot V_j + \nabla_{V_j}(R) = 0, \quad j = 1, 2.$$
 (31)

Equations (30) and (31) may be shown to be equivalent, and either set of equations can be solved to give the flash point.

Similarly, the flash point can be determined by keeping the receiver fixed and moving the source in two nonparallel directions. Therefore, in terms of discrete measurements, the following combinations can be used in order to determine *one* flash point

- I. One source and three noncollinear receivers
- II. Two sources and two receivers, the four being noncollinear
- III. Three noncollinear sources and one receiver.

The method of this section is a global triangulation method, i.e., it completes the triangle with vertices at the source, the receiver, and the flash point. In principle, the complete crack edge can be mapped by using data from one pair of source positions and N pairs of receiver positions. Each pair of receiver positions provides a flash point. Three not necessarily adjacent flash points determine the plane of a flat crack. When we know the plane of the crack, we can determine the tangent at each flash point by the use of (1) or (5). In order that the flash points will not cluster too closely, and in order that a sizable segment of the crack edge will be mapped, the pairs of observation points should be at some distance from each other. Unfortunately, the method is rather sensitive to errors in the input data. It may, however, be expected that a single point close enough to the crack can be determined. This point can then be used as a base point for a local crack-edge mapping, which is discussed in the next section.

The computed position of a flash point will contain errors due to inaccuracies in the data and in the method of computation. The former are the inevitable result of errors in the measurement of the travel time of the first-arriving diffracted signal. The computational errors are incurred in using a finite difference approximation to the gradients $\nabla_U(R)$ and $\nabla_V(R)$. These errors can be illustrated by an application of the inverse method to synthetic diffraction data. In the remainder of this section we consider an example, wherein for a given source, receiver, and crack edge, the ray lengths have been calculated to produce synthetic data. By using this perfect data in the inverse method, the magnitude of the error with increasing source/receiver shifts has been demonstrated. Next, we have introduced artificial errors in the perfect data to show their effect on the computed flash point positions.

Example

Let us consider an ellipse in the plane x = 0, defined by

$$x^2 + 4y^2 - 1 = 0, z = 0.$$
 (32)

Thus, the semi-major axis is unity, and the semi-minor axis is 0.5. Here, the unit length can be chosen arbitrarily, for example, one unit could be 10 m. We consider three positions defined by

1:
$$(9, 1, 10)$$
; 2: $(-3, 7, 10)$; 3: $(-15, 13, 10)$.

These three points serve alternatively as source and receiver positions. The notation (1, 3) means that point 1 is the source and point 3 is the receiver. The exact flash

points are

$$(1, 2): (0.757, 0.327, 0.000)$$
 (33)

$$(1, 3): (-0.041, 0.500, 0.000)$$
 (34)

$$(2, 3)$$
: $(-0.826, 0.282, 0.000)$. (35)

Approximations to the flash points have been found by using method II. The procedure works as follows: at each source/receiver position, a unit vector defined by $(1, 2, 0)/\sqrt{5}$ is taken as the direction of U or V, as the case requires. A shift distance Δv defines the source/receiver pair S_2 , Q_2 corresponding to the original pair S_1 , Q_1 . The four travel times $\tau_{ij}(i, j = 1, 2)$ corresponding to source S_i and receiver Q_j are calculated. A new source position is defined as the mid-point between S_1 and S_2 , and similarly a new receiver point is defined as the mid-point between Q_1

TABLE 1
Positions of Flash Points and Corresponding
Relative Errors for Increasing Shifts of Sources
and Receivers

Δυ	Source Observer	Flash point	Error	
	(1, 2)	(0.757, 0.327, -0.000)	0.000	
0.1	(1, 3)	(-0.041, 0.500, -0.000)	0.000	
	(2, 3)	(-0.826, 0.282, -0.000)	0.000	
	(1, 2)	(0.757, 327, -0.000)	0.001	
0.2	(1, 3)	(~0.042, 0.500, ~0.000)	0.001	
	(2, 3)	(-0.827, 0.282, -0.001)	0.001	
	(1, 2)	(0.755, 0.328, -0.003)	0.004	
0.5	(1, 3)	(-0.044, 500, -0.003)	0.004	
	(2, 3)	(-0.828, 0.282, -0.004)	0.004	
1.0	(1, 2)	(0.746, 0.330, -0.010)	0.015	
	(1, 3)	(0.051, 0.501, -0.012)	0.016	
	(2, 3)	(-0.833, 0.283, -0.016)	0.018	

and Q_2 . With respect to these new positions we have, for example, that

$$\nabla_{U^{(R)}} = c_L(\tau_{21} + \tau_{22} - \tau_{11} - \tau_{12})/2\Delta v + O[(\Delta v)^2]. \tag{36}$$

Thus, the directional derivatives are correct to second order in the shift Δv . The results, stated to three decimal points, are presented in Table 1. The error is defined as the distance between the actual and the computed flash point. Very good agreement is achieved for an intertransducer distance of $\Delta v = 0.1$, but acceptable agreement is still found for $\Delta v = 1$. Whatever value of Δv is taken, the three flash points define a significant segment of the crack edge.

Table 2 shows results for the case of various uniform ray length errors. Not unexpectedly, ray length errors of unity can introduce errors in the flash point positions of the order of 0.5, i.e., of the order of the semi-minor axis of the ellipse. If the unit is 10 m, and we consider a velocity of $c_L = 6.10^3$ m/sec, a ray length error

of a unit corresponds to an error in the time measurement of about 0.0015 sec. It is apparent that the global triangulation method can give rise to substantial errors if it were to be used for the mapping of the complete crack edge, and if the errors were uniform for each set of data, but quite different for different data sets.

The uniform ray length errors considered do not produce a sizable error in the computed directional derivative, but rather, have the effect of spatially translating the flash points. However, if the errors are allowed to be nonuniform for the same data set, the gradient approximation can become very erroneous, leading to much larger errors for the computed flash points. In the next section, we present results for the alternate method proposed in this paper, the local crack-edge mapping, for the case of random errors.

LOCAL CRACK-EDGE MAPPING

The global triangulation method can be used to determine a point on or near the crack edge. In this section, it is shown that such a point can subsequently be used

TABLE 2
FLASH POINT ERRORS (FPE) FOR INCREASING RAY
LENGTH ERRORS (RLE) AND INCREASING SHIFTS OF
SOURCES AND RECEIVERS

Δυ	Source	rie = 0.5	rle = 1.0	rle = -1.0
	Observer	fpe	fpe	fpe
0.1	(1, 2)	0.295	0.587	0.596
	(1, 3)	0.387	0.766	0.798
	(2, 3)	0.356	0.717	0.700
	(1, 2)	0.295	0.587	0.596
0.2	(1, 3)	0.387	0.766	0.798
	(2, 3)	0.356	0.716	0.699
	(1, 2)	0.297	0.590	0.594
0.5	(1, 3)	0.388	0.768	0.796
	(2, 3)	0.354	0.715	0.700
1.0	(1, 2)	0.305	0.600	0.586
	(1, 3)	0.394	0.773	0.791
	(2, 3)	0.350	0.711	0.704

as a base point. Relative to the base point other points on the crack edge can be determined by a local crack-edge mapping. The local mapping is also based on travel times from source to receiver via a flash point. However, instead of using single travel times to produce single flash points, we now use a set of travel times to simultaneously produce a set of flash points. The local crack-edge mapping should have greater accuracy than the global triangulation method.

As before, we have a source S at x_S and a receiver Q at x_Q . The travel time τ for the diffracted signal is assumed known. Then the flash point x_D lies on the surface E defined by equation (13). The unit vectors \mathbf{p} and \mathbf{q} and the distances R_i and R_L are defined by equations (11) and (12). With respect to the base point B, whose position is defined by x_B , we define the unit vectors \mathbf{p}_B and \mathbf{q}_B , and the distances R_{SB} , R_{QB} , and R_B as follows

$$x_B = x_S + R_{SB} \boldsymbol{p}_B = x_Q + R_{QB} \boldsymbol{q}_B \tag{37}$$

$$R_B = R_{SB} + R_{QB}. \tag{38}$$

The geometry is shown in Figure 3.

Now, we consider

$$c_{LT} - R_B = R - R_B = R_i - R_{SB} + R_L - R_{QB}. \tag{39}$$

Since

$$R_i - R_{SB} \simeq (\mathbf{x}_D - \mathbf{x}_B) \cdot \mathbf{p}_B \tag{40}$$

$$R_L - R_{QB} \simeq (\mathbf{x}_D - \mathbf{x}_B) \cdot \mathbf{q}_B, \tag{41}$$

equation (39) yields

$$(\mathbf{x}_D - \mathbf{x}_B) \cdot (\mathbf{p}_B + \mathbf{q}_B) \simeq c_L \tau - R_B. \tag{42}$$

Equation (42) represents a plane which approximates the surface E near the flash point D.

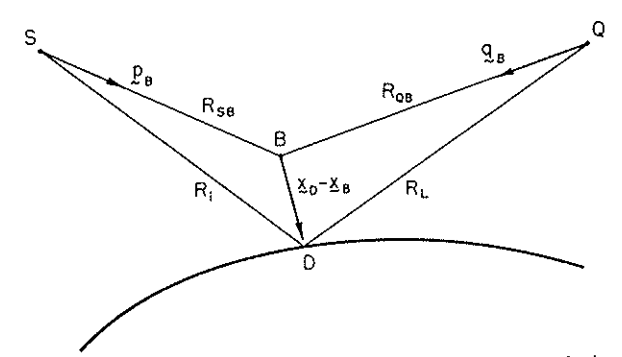


Fig. 3. Base point B near crack edge for local mapping technique.

To map the edge of a crack, we consider n source positions S_i , i = 1, n and m observer positions Q_j , j = 1, m. For each source observer pair (S_i, Q_j) , there is an associated travel time, which provides an input to equation (42). The base point defined by x_B remains the same for all cases. The planes that are obtained in this manner pass very close to the crack edge, in fact they envelope a curve which is an approximation to a segment of the crack edge. The inversion thus reduces to finding the congruence of all the planes. Since our data are finite, we will obtain a polygon of points which approximates a segment of the crack edge.

For specificity, we consider the case that there are two sources and 20 receivers. The corresponding travel times give 40 planes of the type defined by (42). Let $\Omega(i,j)$, i=1,2,j=1, 20 be such a set of planes. Points on the crack edge may be found as follows: consider the intersection of the planes $\Omega(1,j)$, j=1, 20 with any one of the planes $\Omega(2,j)$, j=1, 20, say $\Omega(2,k)$. The locus of intersection is a polygon, which we denote by $\Gamma(2,k)$. To obtain points which approximate the flash points, we test to see if any of the planes $\Omega(2,j)$, $j\neq k$ intersect the polygon $\Gamma(2,k)$. For such a point of intersection to exist, the flash point of $\Omega(2,j)$ at j=k must be interspersed with the flash points of $\Omega(2,j)$, j=1, 20, $j\neq k$. Also, we require that the segment of the crack edge containing the flash points of $\Omega(1,j)$, j=1, 20 has a section in common with the segment for the planes $\Omega(2,j)$, j=1, 20.

In the general procedure, we first obtain three points in order to specify the plane of the crack. Once this has been achieved, the remaining approximate flash points are easily determined as being on the polygon formed by the set of planes $\Omega(i,j)$, $i=1,\,2,\,j=1,\,20$ and the crack plane. Since the accuracy is unknown, an iterative procedure should be used. In this procedure, a new initial point is taken, say at one of the estimated flash points. Then the mapping procedure is repeated. In general, such an iteration can be performed several times until all the points converge to fixed points on the edge.

Example

The same ellipse in the z=0 plane described by equation (32) is considered. The two source positions and the array of 20 receiver positions are all taken in the plane

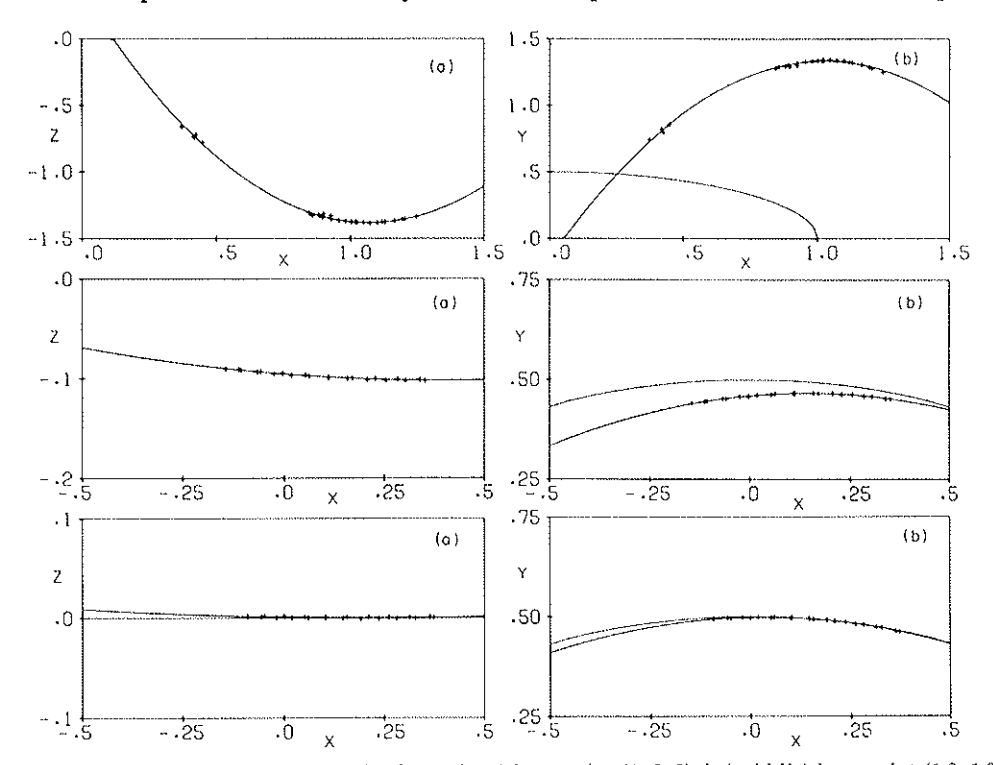


Fig. 4. Computed points and crack edge: a (top) base point (1, 3, 3); b (middle) base point (1.2, 1.3, 1.2); and c (bottom) base point (0.2, 0.5, 0).

z = 10. The x, y coordinates are

$$S_1$$
: (-10, 10), S_2 : (-5, 10), $Q_j = (5, 20) + j(0.5, -0.75), $j = 1, 20.$$

In a trial calculation, the point (1, 3, 3) was arbitrarily chosen as the initial base point. Figure 4 shows the projections of the computed points on the planes y = 0(a) and z = 0(b), respectively. A least-square quadratic fit is plotted through the points. The actual crack edge is also shown. Very poor agreement is noted for this base point. For the first iteration, one of the cluster of points in Figure 4a was chosen as a new base point, namely (1.2, 1.3, 1.2). The results, shown in Figure 4b are seen to be much closer to the crack edge. From these points, we select the base point (0.2, 0.5, 0) and proceed with the next iteration to obtain Figure 4c.

Figure 5 shows the same results for the case that the synthetic travel times (or

ray lengths) have been perturbed with random errors. The error in the ray length was taken at random from (-0.01, 0.01) for each ray path between source S_i and receiver Q_j ; i = 1, 2, j = 1, 20. It is observed that the points do not define a curve as

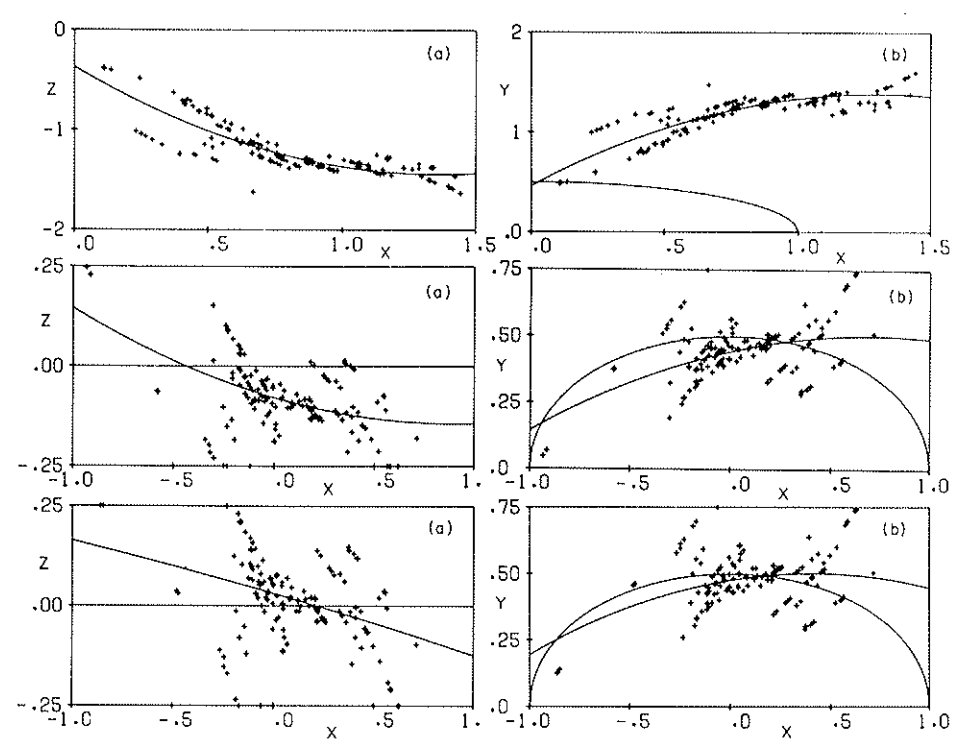


Fig. 5. Computed points and crack edge for random errors of ray lengths in range (-0.01, 0.01); a (top) base point (1, 3, 3); b (middle) base point (1.2, 1.3, 1.2); and c (bottom) base point (0.2, 0.5, 0).

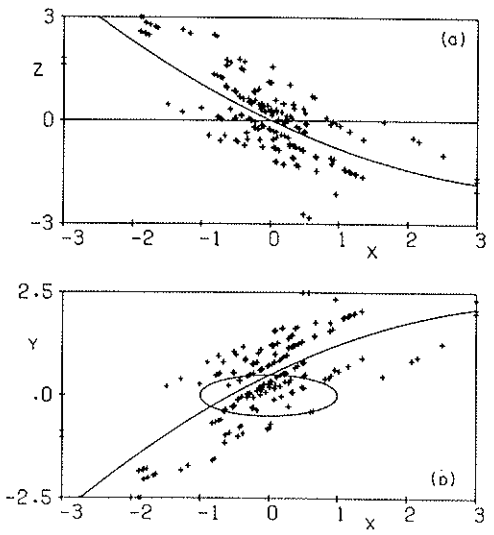


Fig. 6. Computed points and crack edge for random errors of ray lengths in range (-0.05, 0.05), base point (0.2, 0.5, 0).

clearly as in the case of error-free data. However, the least-square quadratic fit gives a reasonable approximation. If a random error between -0.05 and +0.05 is allowed (see Figure 6), then there is no discernible edge present in the computed points.

This suggests that an error between 0.01 and 0.05 is an upper limit on the magnitude of permissible random errors in the ray length. If one unit is 10 m and the velocity is $c_L = 6.10^3$ m/sec, the error 0.01 translates into a time error of 15 μ sec.

We note that the errors considered here are random, as opposed to the uniform errors considered in the previous section for the global triangulation method. Uniform errors have the same net effect on the local edge mapping as on the global triangulation, i.e., the edge will be translated by an amount which is approximately proportional to the error.

ACKNOWLEDGMENT

The first phase of this work was sponsored by the Los Alamos Scientific Laboratory under Contract N68-8539G-1. The paper was completed in the course of research sponsored by the U.S. Army Research Office (Durham) under Grant DAAG29-80-C-0086.

REFERENCES

- Achenbach, J. D. and A. K. Gautesen (1977). Geometrical theory of diffraction for 3-D elastodynamics, J. Acoust. Soc. Am. 61, 413-421.
- Achenbach, J. D., A. K. Gautesen, and H. McMaken (1978). Diffraction of point-source signals by a circular crack, *Bull. Seism. Soc. Am.* 68, 889-905.
- Achenbach, J. D., L. Adler, D. K. Lewis, and H. McMaken (1979). Diffraction of ultrasonic waves by penny-shaped cracks in metals: theory and experiment, J. Acoust. Soc. Am. 66, 1848-1856.
- Brown, M. C., R. B. Duffield, C. L. B. Siciliano, and M. C. Smith (1978). Hot Dry Rock Geothermal Energy Development Program (Annual Report 1978), LA-7807-HDR, Los Alamos Scientific Laboratory, Los Alamos, New Mexico.
- Fehler, M. and K. Aki (1978). Numerical study of diffraction of plane elastic waves by a finite crack with application to location of a magma lens, *Bull. Seism. Soc. Am.* 68, 573-598.
- Norris, A. N. and J. D. Achenbach (1982). Mapping of a crack edge by ultrasonic methods, J. Acoust. Soc. Am. (in press).
- Salvado, C. and J. B. Minster (1980). Slipping interfaces: a possible source of S radiation from explosive sources, Bull. Seism. Soc. Am. 70, 659-670.

DEPARTMENT OF CIVIL ENGINEERING NORTHWESTERN UNIVERSITY EVANSTON, ILLINOIS 60201

Manuscript received 16 March 1981

	1			
	:			

